*J Physiol* (2003), **553.2**, *pp.* 473–488
DOI: 10.1113/jphysiol.2003.051110

www.jphysiol.org

*Journal of Physiology*

# Decoding of synaptic voltage waveforms by specific classes of recombinant high-threshold $Ca^{2+}$ channels

Zhi Liu*§, Jihong Ren*§ and Timothy H. Murphy*†‡§

**Kinsmen Laboratory and Brain Research Centre, Departments of †Psychiatry and ‡Physiology, §Graduate Program in Neuroscience, University of British Columbia, Vancouver, BC, Canada*

**Studies suggest that the preferential role of L-type voltage-sensitive $Ca^{2+}$ channels (VSCCs) in coupling strong synaptic stimulation to transcription is due to their selective activation of local chemical events. However, it is possible that selective activation of the L-type channel by specific voltage waveforms also makes a contribution. To address this issue we have examined the response of specific $Ca^{2+}$ channel types to simulated complex voltage waveforms resembling those encountered during synaptic plasticity (gamma and theta firing frequency). L-, P/Q- and N-type VSCCs ($\alpha_{1C}$, $\alpha_{1A}$, $\alpha_{1B}/\beta_{1B}/\alpha_{2\delta}$, respectively) were all similarly activated by brief action potential (AP) waveforms or sustained step depolarization. When complex waveforms containing large excitatory postsynaptic potentials (EPSPs), APs and spike accommodation were applied under voltage clamp we found that the integrated L-type VSCC current was approximately three times larger than that produced by the P/Q- or N-type $Ca^{2+}$ channels (gamma frequency 1 s stimulation). For P/Q- or N-type channels the complex waveforms led to a smaller current than that expected from the response to a simple 1 s step depolarization to 0 or +20 mV. EPSPs present in the waveforms favoured the inactivation of P/Q- and N-type channels. In contrast, activation of the L-type channel was dependent on both EPSP- and AP-mediated depolarization. Expression of P/Q-type channels with reduced voltage-dependent inactivation ($\alpha_{1A}/\beta_{2A}/\alpha_{2\delta}$) or the use of hyperpolarized intervals between AP stimuli greatly increased their response to complex voltage stimuli. We propose that in response to complex synaptic voltage waveforms P/Q- and N-type channels can undergo selective voltage-dependent inactivation leading to a $Ca^{2+}$ current mediated predominantly by L-type channels.**

(Received 14 July 2003; accepted after revision 12 September 2003; first published online 18 September 2003)
**Corresponding author** T.H. Murphy: Department of Psychiatry, 4N1-2255 Wesbrook Mall, Vancouver, BC, Canada V6T 1Z3.
Email: thmurphy@interchange.ubc.ca

A combination of molecular biological and electrophysiological characterization studies has revealed a significant degree of structural and functional heterogeneity for the different voltage-sensitive $Ca^{2+}$ channel (VSCC) types (Zhang *et al.* 1993; Ertel *et al.* 2000). Broadly, VSCCs fall into two categories based on their physiological and pharmacological profiles (Zhang *et al.* 1993). The first category includes VSCCs that require high levels of depolarization for their activation and includes the L-, P/Q-, N- and R-types. The second category is composed solely by T-type VSCCs and requires lower levels of depolarization for activation. More recent nomenclature gives rise to three structurally and functionally related families ($Ca_v1$, $Ca_v2$ and $Ca_v3$) (Ertel *et al.* 2000). The L-, P/Q- and N-type channels in our study correspond to $Ca_v1.2$, $Ca_v2.1$ and $Ca_v2.2$ respectively. R-type currents can be attributed in part to $\alpha_{1E}$ subunit ($Ca_v2.3$). The low-threshold activated T-type channel corresponds to the $Ca_v3$ family and consists of three channel types, $Ca_v3.1$, $Ca_v3.2$ and $Ca_v3.3$. The subunit composition of the different VSCCs also varies and has dramatic effects on channel inactivation (Stotz & Zamponi, 2001). L-, P/Q- and N-type channels display varying degrees of $Ca^{2+}$- and voltage-dependent inactivation, whereas the L-type channel undergoes predominantly $Ca^{2+}$-dependent inactivation (Yue *et al.* 1990; Randall & Tsien, 1995). Experimental evidence suggests a selective role for L-type VSCCs in activating immediate early gene expression in response to stimuli that mimic robust synaptic stimulation (Murphy *et al.* 1991; Bading *et al.* 1993; Dolmetsch *et al.* 2001; Weick *et al.* 2003). The preferential role of the L-type channel is thought to result from its selective coupling to intracellular signal transduction pathways triggered by specific spatial and temporal properties of $Ca^{2+}$ signalling (Murphy *et al.* 1991; Bading *et al.* 1993; Dolmetsch *et al.* 2001; Weick *et al.* 2003). However, it is also possible that selective activation of the L-type channel in response to particular voltage stimuli in combination with local $Ca^{2+}$-dependent chemical events provides an even more selective mechanism for stimulus–transcription coupling. The biophysical properties of the L-type VSCC, including its

relatively slow inactivation (Zhang *et al.* 1993), suggest that it is an ideal sensor for long-lasting bursts of activity that lead to steady depolarization (Nakazawa & Murphy, 1999; Mermelstein *et al.* 2000). We have extended these previous studies by performing voltage-clamp experiments on recombinant L-, P/Q- and N-type VSCCs expressed in human embryonic kidney (HEK) 293 cells using complex waveforms that mimic synaptic stimuli at physiological temperature as voltage commands.

Our experiments involve first producing plausible EPSP and AP waveforms using a computer simulation of CA1 hippocampal neuron synaptic physiology and then testing whether specific VSCC subtypes are tuned to these physiologically relevant waveforms (i.e. gamma and theta firing frequencies) (Christie *et al.* 1995*b*; Thomas *et al.* 1998). Surprisingly, our initial experiments at physiological temperature and with $Ca^{2+}$-dependent inactivation present indicate little difference in the response of L-, P/Q- and N-type channel types to prolonged step depolarization (1 s). Therefore, we set out to determine whether differential activation of VSCC subtypes might occur under conditions of physiological temperature and divalent ion concentration in response to complex voltage waveforms that more closely mimic synaptic stimuli. Under these conditions we observed that complex synaptic burst waveforms led to a selective voltage-dependent inactivation of non-L-type VSCCs that was not readily predicted by the response of the channels to simple prolonged step depolarization. This selective inactivation process leads to a $Ca^{2+}$ current with a significantly larger L-type component. We suggest that the tuning of L-type channels to specific voltage waveforms, together with their preferential link to intracellular signal transduction, collaborate to give the channels a unique role in coupling synaptic stimulation to transcriptional activation (Murphy *et al.* 1991; Bading *et al.* 1993; Dolmetsch *et al.* 2001).

## METHODS

### Hippocampal CA1 neuron model

We performed our simulation with the program NEURON (version 4.1.1) (Hines & Carnevale, 1997) on a PII-450 PC, using a 25 $\mu$s time step. The purpose of the model was to create plausible somatic waveforms for pyramidal neuron activity during high-frequency stimulation. Simulated recording have inherent advantages including the ability to easily alter stimulation frequency or particular conductance.

Studies by Mainen & Sejnowski (1998) indicate that the complex spiking behaviour of pyramidal neurons can be modelled using relatively few compartments. For our CA1 neuron model we have used four compartments that include a central soma as well as two dendritic processes and an axon. The model cell has the following passive membrane parameters: axial resistance ($R_a$) = 100 Ω cm (for dendrites and soma, 50 Ω cm for axon), membrane resistance ($R_m$) = 50 000 Ω cm$^2$, membrane capacitance ($C_m$) = 1 $\mu$F cm$^{-2}$. Conductances were placed in these various compartments at levels indicated based on experimental data (see Table 3, Appendix). To simplify the model, synaptic conductances were placed along the dendrites at 100, 300 and 700 $\mu$m positions. The axon hillock was defined as a short segment between the axon and the soma. To simulate a lower threshold for AP initiation within the axon hillock region we have added a higher concentration of voltage-gated $Na^+$ conductance. Although this results in back-propagating APs, it is possible that in actual neurons there are alternative mechanisms (Colbert & Pan, 2002).

A notable feature of hippocampal CA1 pyramidal neurons is the presence of back-propagating APs (Spruston *et al.* 1995; Stuart *et al.* 1997*b*). Recent data suggest that a gradient (highest in distal regions) of dendritic A-type $K^+$ current ($I_A$) also plays an important role in attenuating dendritic back-propagating APs in hippocampal CA1 neurons (Hoffman *et al.* 1997). Accordingly, we have included a gradient of $I_A$ expression as in Hoffman *et al.* (1997). To study the activation of VSCCs during stimuli that are relevant to synaptic plasticity, we have modelled the effect of 100 Hz trains of presynaptic stimulation on postsynaptic membrane potential in the soma. Our experimental data suggest that hippocampal CA1 neurons exhibit a complex firing behaviour in response to 100 Hz tetanic stimulation (data not shown). Notable features of the response to tetanic stimulation include spike accommodation as well as voltage-dependent inactivation of $Na^+$ currents (Fleidervish *et al.* 1996; Mickus *et al.* 1999). These two phenomena lead to a slowing of AP frequency and a reduction in amplitude. It has been reported that in hippocampal CA1 neurons, one type of voltage-activated $K^+$ channel ($I_M$) and three types of $Ca^{2+}$-activated $K^+$ channels (BK, s$I_{AHP}$ and SK) are responsible for the spike frequency accommodation (Sah & Bekkers, 1996; Halliwell & Adams, 1982; Shao *et al.* 1999). The properties of these $K^+$ channels were modelled according to reported experimental data. To produce voltage-dependent inactivation of $Na^+$ channels we added a slow variable, *s*, into the classical Hodgkin–Huxley-type $Na^+$ channel model and were able to obtain a frequency- and voltage-dependent inactivation of $Na^+$ channels during AP trains (Mickus *et al.* 1999). Comparison of simulated 100 Hz synaptic stimulus trains (Fig. 2) to experimental data from hippocampal pyramidal neurons (Egorov *et al.* 1999; Yeckel *et al.* 1999) indicates good qualitative correspondence. One of the most critical parameters for generation of different firing patterns is the level of synaptic conductance, which represents the combined open channel conductance of all NMDA and AMPA receptors. The synaptic conductance of the model was set to 0.0075 $\mu$S to generate a single AP and was increased to 0.01 and 0.3 $\mu$S to produce the repetitive and plateau waveforms respectively (100 Hz presynaptic stimulation). Theta stimulation was produced by delivering presynaptic burst stimulation with a 7.5 Hz frequency and either a strong or a weak synaptic conductance (0.01 and 0.3 $\mu$S). GABAergic mechanisms were not included in the model (see Appendix for more detailed mechanisms).

### Preparation of HEK 293 cells

HEK 293 cells (CRL 1573; ATCC, Rockville, MD, USA) were passaged once every 2–4 days. For calcium phosphate transfection cells were plated at a density of 1 × 10$^6$ cells ml$^{-1}$ in 10 cm culture dishes (Falcon, Becton Dickinson Labware, Franklin Lakes, NJ, USA). Cells were transfected for 6–8 h with cDNAs encoding the rat brain $\alpha_1$ ($\alpha_{1A}$ or $\alpha_{1C}$), $\alpha_{2\delta}$ and $\beta$ subunit ($\beta_{1B}$ or $\beta_{2A}$) (obtained from Dr T. Snutch, University of British Columbia, Canada) at a ratio of 1:1:1 with a total of 12 $\mu$g plasmid cDNA for a 10 cm culture plate. After a period of 16–24 h following transfection,

cells were transferred to a 29 °C incubator (in some experiments 37 °C) for up to 5 days (Stotz & Zamponi, 2001). Recordings were initiated 36 h after the termination of transfection. For the N-type VSCC, the HEK tsa201 cell line stably expressing $\alpha_{1B}$, $\alpha_{2\delta}$ and $\beta_{1B}$ subunits (obtained from Dr Snutch) was used. The N-type channel $\alpha$ subunit (rbB-II isoform) was in the unmodulated G177 form, which features the 'willing' state with fast activation and susceptibility to G-protein inhibition (Zhong *et al.* 2001). Our $\alpha_{1A}$ construct represents a splice variant of $\alpha_{1A\text{-}a}$ subtype, which is missing both a valine insertion ($Val_{421}$) in I–II linker as in P-like channels and the insertion of asparagine plus proline (N1605–P1606) into the S3–S4 extracellular linker of repeat IV as in Q-like channels (Bourinet *et al.* 1999). This $\alpha_{1A\text{-}a}$ subtype may correspond to a novel P-like channel in the cerebellum with a functional profile intermediate between P- and Q-like channels (Tottene *et al.* 1996).

### Electrophysiology

Voltage-clamp recording was performed at both room temperature (21.5–23 °C) and physiological temperature (35–37.5 °C) on the stage of an inverted microscope (Aviovert, Zeiss). Electrodes with open tip resistances of 1–3 MΩ after routine Sylgard coating and fire polishing were used. The extracellular recording solution for the HEK 293 cells contained (mM): 2 $CaCl_2$, 1 $MgCl_2$, 145 $TEAMeSO_3$ and 10 Hepes (pH 7.35 adjusted with TEA-OH) with osmolarity adjusted to 300 mosmol $l^{-1}$. The intracellular recording solution for the HEK 293 cells contained (mM): 120 $CsMeSO_3$, 5 CsCl, 10 EGTA, 1 $MgCl_2$, 4 MgATP, 0.3 NaGTP and 10 Hepes (pH 7.3, CsOH) with osmolarity adjusted to 290 mosmol$^{-1}$. Currents were sampled at 10 kHz, filtered at 5 kHz and acquired and analysed using pCLAMP software and an Axopatch 200A amplifier (Axon Instruments, Foster City, CA, USA). Pipette series resistance was between 2–5 MΩ. Typically 75 % series resistance compensation was obtained and a *P*/4 leak subtraction protocol was performed for all the recordings. In general we expect that AP-like voltages were delivered properly since we estimate voltage-clamp time constants (expressed as $R_{a,eff}C_m$ ($R_{a,eff}$: effective access resistance) to be less than 50 $\mu$s and thus considerably faster than the 10 kHz sampling rate used. To check the speed of clamp on individual cells we examined the rise time of the tail current and found it to be 0.14 ± 0.01 ms ($n$ = 28 cells).

To overcome increased rundown apparent at physiological temperature, no more than four waveforms were applied in less than 3 min. The waveform sequence was randomized and preceded routinely by a step pulse to monitor current rundown. Given that different preparations of HEK 293 cells can express different levels of channels we have normalized the VSCC responses (to particular waveforms) of each cell to a measure of peak VSCC activity. To estimate the peak channel activity we produced long steady depolarizations (> 50 ms step pulses) to membrane potentials expected to maximally activate a particular channel type. For the L- and P/Q-type channels 0 mV was used. Since the N-type channel had a more positive activation potential the amplitude of the current evoked by a step to +20 mV was used (Fig. 1). The leak-subtracted currents were then integrated over the 1 s period of simulated train stimulation (result expressed in picocoulombs, pC). The integral was then divided by the peak current amplitude of the step pulse and the result was expressed in units of pC $nA_{peak}^{-1}$. One-way ANOVA and two-tailed paired and unpaired $t$ tests (as appropriate) were performed to evaluate significance of differences between group means (expressed as means ± S.E.M.); $n$ refers to the number of cells recorded from.

## RESULTS

### L-, P/Q- and N-type voltage sensitive $Ca^{2+}$ channels all respond to brief action potential-like stimuli

Using simulated AP and EPSP waveforms as voltage commands (McCobb & Beam, 1991; Patil *et al.* 1998), we have conducted whole-cell voltage-clamp experiments on HEK 293 cells expressing different recombinant VSCCs. We have contrasted the activation of the $\alpha_{1A}$ (P/Q-type), $\alpha_{1B}$ (N-type) and $\alpha_{1C}$ (L-type) subunits expressed in combination with the $\beta_{1B}$ (or in some cases $\beta_{2A}$) and $\alpha_{2\delta}$ subunits. To perform our experiments under more physiological conditions we elevated the bath temperature to ~37 °C (range 35–37.5 °C) and observed a marked increase in the activation rate as well as a speeding of inactivation of all channel types (see Fig. 1*A* and *B*, Tables 1 and 2). In these experiments we used 2 mM $Ca^{2+}$ as the charge carrier for characterization of VSCCs and the expression of the $\beta_{1B}$ subunit to preserve voltage and $Ca^{2+}$-dependent inactivation expected under physiological conditions in neurons (Pragnell *et al.* 1991; Ludwig *et al.* 1997). The peak current was also significantly increased (> 300 %) compared to responses recorded at room temperature (22 °C) for the three channel types studied (Table 1). Surprisingly, we found that the three channel types at 37 °C produced qualitatively similar responses to the strong step depolarization (Fig. 1*A* and *B*). At 37 °C less than a 40 % difference in the integrated $Ca^{2+}$ current over a 1 s period was observed when L-, P/Q- and N-type channels were compared (data normalized to peak response, see Methods). Elevated temperature was also associated with a hyperpolarizing shift in the voltage at which half-maximal channel activation occurred for L- and P/Q-type channels ($V_{½\,act}$: 22/37 °C; L: −10.2 ± 3.1/−20.0 ± 1.3 mV; P/Q: −12.6 ± 0.9/−23.2 ± 1.2 mV; and N: 6.2 ± 1.5/5.5 ± 2.6 mV; see Fig. 1*C* for 37 °C data). The conductances were fit to the Boltzmann equation (Tateyama *et al.* 2001) and the $V_{½}$ was determined. The reversal potentials used for calculating the conductance were 50.7 ± 1.8 mV ($n$ = 12), 49.4 ± 1.8 mV ($n$ = 14) and 53.1 ± 2.4 mV ($n$ = 12) for L-, P/Q- and N-type channels respectively. L-type VSCCs were markedly more resistant to steady-state inactivation than the P/Q- or N-type; 50 % channel inactivation at −64 mV for both P/Q- and N-type *versus* −35 mV for L-type VSCCs (Fig. 1*D*). The voltage dependence of inactivation was similar to published values for P/Q- and N-type channels (Patil *et al.* 1998; Sutton *et al.* 1999). In this study, we have termed the inactivation state at the end of a 1 s step depolarization 'steady-state inactivation', although it is possible that a more slowly developing component (< 10 % amplitude) may also be involved.

Previous studies have suggested that L-type VSCCs respond preferentially to a large long-lasting depolarization and do not respond as well to brief stimuli such as single APs (Murphy *et al.* 1991; Mermelstein *et al.* 2000).

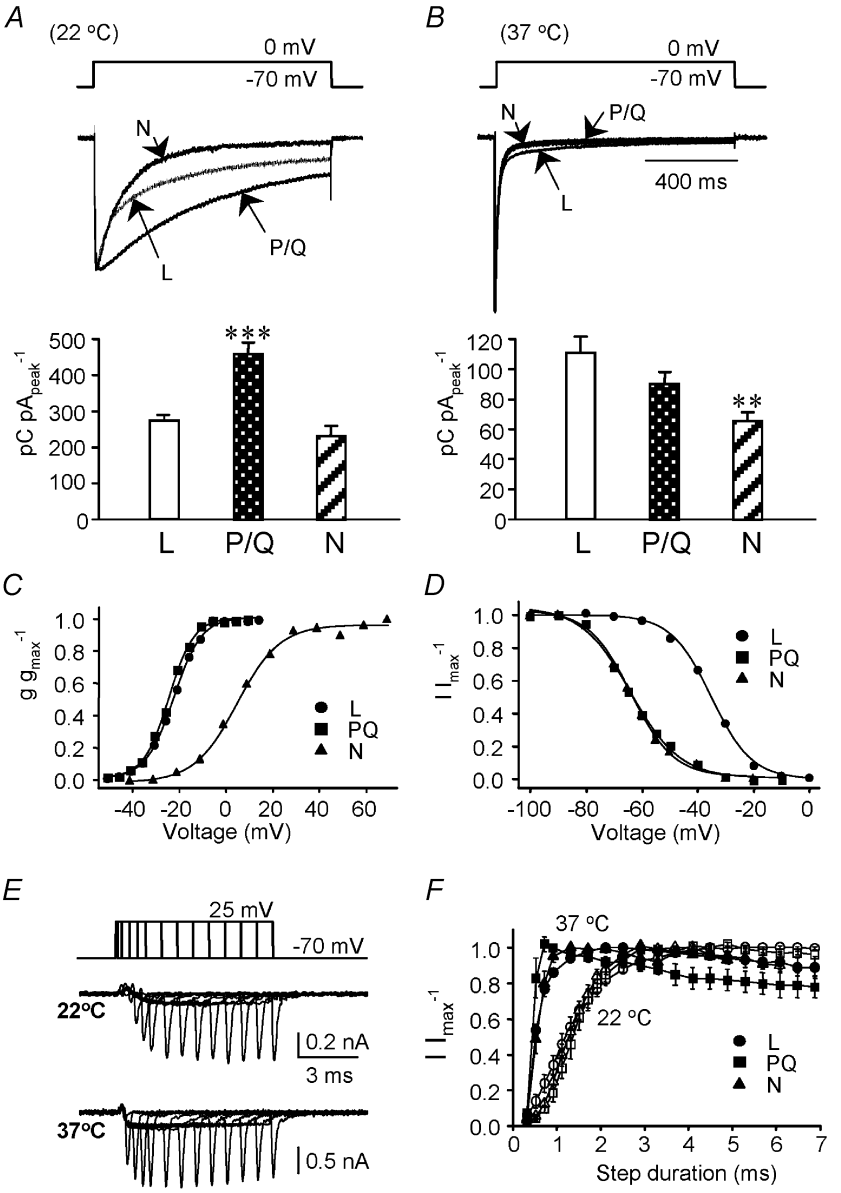


**Figure 1. Activation and inactivation of VSCCs in response to step depolarization**

*A*, at room temperature (~22 °C) L-, P/Q- and N-type channels expressed in HEK 293 cells have relatively slow activation and inactivation kinetics (1 s step depolarization from −70 to 0 mV, except +20 mV for N-type). *B*, at 37 °C all three channel types studied exhibited dramatically faster activation and inactivation. Overplotted normalized records (to peak current) of L-, P/Q- and N-type VSCC currents in response to the 1 s step depolarization are shown in *A* and *B*. Group data indicate that the normalized integrated L-type VSCC current (integral in pC divided by peak current; pC $pA_{peak}^{-1}$) is only moderately larger than the other two channel types in response to the 1 s depolarization (significant difference between the L- and N-type channels; $P < 0.01$ one-way ANOVA). For this analysis the currents were integrated over the 1 s waveform and normalized to the peak current ($n = 17$, 21 and 14 for L-, P/Q- and N-type respectively). *C*, voltage dependence of L-, P/Q- and N-type channel activation at 37 °C determined by monitoring the peak current response at the indicated potentials and expressing the data as a conductance change ($g\,g_{max}^{-1}$). The conductances were fit to the Boltzmann equation and the $V_{½}$ was determined. *D*, channel inactivation determined by a 10 ms test pulse from −100 to 0 mV given 2–5 ms after a 1 s inactivating step to 0 mV from the indicated holding potentials. The peak currents elicited at 0 mV were then normalized to the maximal response obtained and fitted to the Boltzmann equation to determine the voltage at which 50 % of the channels were inactivated: P/Q- (−64 mV, $n = 5$) and N-type $Ca^{2+}$ channels (−64 mV, $n = 8$) have a markedly more negative inactivation profile than L-type channels (−35 mV, $n = 7$). *E*, step pulses of limiting duration indicate that APs effectively activate L-, P/Q- and N-type channels. A series of short step depolarizing pulses from −70 to +25 mV of varied duration from 0.1 to 3.1 ms were given to mimic APs of varying duration. An example of an overplotted L-type VSCC response to the short step pulses at 22 and

**Table 1. Characteristics of L-, P/Q- and N-type VSCCs derived from 1 s step depolarization**

| | | Rise time (ms) | | Peak (pA) | | Residual ratio (%) | |
|---|---|---|---|---|---|---|---|
| | | 22 °C | 37 °C | 22 °C | 37 °C | 22 °C | 37 °C |
| L | $\beta_{1B}$ | 3.2 ± 0.2 | 0.6 ± 0.03 | −506 ± 114 | −2354 ± 470 | 14.9 ± 1.1 | 6.2 ± 1.0 |
| | | $n$ = 18 | $n$ = 24 | $n$ = 10 | $n$ = 24 | $n$ = 7 | $n$ = 11 |
| | $\beta_{2A}$ | — | 0.4 ± 0.1 | — | −1259 ± 423 | — | 16.0 ± 2.0 |
| | | | $n$ = 5 | | $n$ = 5 | | $n$ = 5 |
| P/Q | $\beta_{1B}$ | 13.4 ± 0.9 | 0.3 ± 0.02 | −345 ± 43 | −1306 ± 240 | 24.9 ± 4.0 | 2.7 ± 0.4 |
| | | $n$ = 9 | $n$ = 9 | $n$ = 9 | $n$ = 9 | $n$ = 9 | $n$ = 8 |
| | $\beta_{2A}$ | — | 0.5 ± 0.03 | — | — | — | 32.5 ± 2.6 |
| | | | $n$ = 6 | | | | $n$ = 5 |
| N | $\beta_{1B}$ | 2.3 ± 0.7 | 0.5 ± 0.04 | — | −845 ± 154 | — | 2.2 ± 0.5 |
| | | $n$ = 4 | $n$ = 15 | | $n$ = 15 | | $n$ = 14 |
| | $\beta_{2A}$ | — | 1.1 | — | −520 | — | 63.5 |
| | | | $n$ = 1 | | $n$ = 1 | | $n$ = 1 |

VSCC, voltage-sensitive $Ca^{2+}$ channel. The rise times between 22 and 37 °C were significantly different for all channel types studied ($P < 0.001$). The residual ratio is the percentage of steady-state current value at the end of 1 s depolarization over the step peak current. $\alpha_{1A}$ (P/Q-type), $\alpha_{1B}$ (N-type), and $\alpha_{1C}$ (L-type) subunits were expressed in HEK 293 cells in combination with $\beta_{1B}$ or $\beta_{2A}$ and $\alpha_{2\delta}$ subunits.

However, these studies were limited in that they were performed on a heterogeneous population of channels at room temperature. The studies also failed to describe how L-type VSCCs are activated by bursts of APs and EPSPs associated with synaptic plasticity (Christie *et al.* 1995*b*; Thomas *et al.* 1998). Under more physiological conditions, neurons would rarely experience steady depolarization in the form of EPSPs to potentials more positive than −40 mV (Storm & Hvalby, 1985). To further address this issue, voltage steps (to +25 mV) of different lengths were used to simulate APs of limiting duration (Fig. 1*E*). At 22 °C we observed that step widths of < 1 ms resulted in < 50 % of maximal channel activation for L-, P/Q- and N-type channels. However, at 37 °C we observed that all three channel types were effectively activated (up to 90 %) by AP mimicking steps of ~1.0 ms (Fig. 1*E* and *F*). Using briefer pulses (< 0.5 ms) we observed that the P/Q-type channel was more effectively activated than the N- or L-type channels ($P < 0.05$), consistent with the shorter rise time of the P/Q-type channel at 37 °C shown in Table 1.

### Selective response of L-type voltage-sensitive $Ca^{2+}$ channels to simulated gamma and theta frequency synaptic activity

In contrast to the effect of step depolarization, application of more complex and physiologically relevant simulated waveforms, corresponding to 1 s of gamma and theta presynaptic stimuli, led to marked differences in VSCC kinetics and in integrated current (over 1 s) when the three channel types were compared (Fig. 2*A* and *B*). In simulating the postsynaptic (somatic) response of a CA1 hippocampal neuron to high-frequency presynaptic stimulation we included mechanisms responsible for many of the salient features of postsynaptic activity including spike accommodation, EPSPs and $Na^+$ channel inactivation. To control for differences in absolute expression levels we normalized the area of the $Ca^{2+}$ current for the test waveforms to the peak amplitude of a preceding step response in which maximal channel activation occurred (see Methods). The normalized integrated $Ca^{2+}$ current through the L-type VSCC in response to a complex waveform containing both EPSPs and APs (termed the repetitive firing waveform, reflects postsynaptic EPSPs and APs stimulated by a 100 Hz presynaptic tetanus) was considerably larger than that mediated by the P/Q- or N-type VSCC (335 and 518 % of the P/Q- and N-type responses respectively; see Fig. 2*A* and *B*). To stimulate more robust levels of depolarization we also simulated a plateau-type waveform by increasing the simulated synaptic conductance (30-fold). In this case the simulated neuron was depolarized to a steady level of −33 mV and again the integrated L-type response was considerably better than the P/Q-type or the N-type (288 %, and 679 % of the P/Q- and N-type responses respectively; see Fig. 2*A* and *B*). In response to the plateau much of the current entry through the L-type VSCC as well as the difference in total $Ca^{2+}$ influx between channel types was associated with the plateau itself and appeared as a

37 °C. A steady $Ca^{2+}$ current as well as a large transient tail current was observed. *F*, group data showing the responses of all 3 channel types; open symbols indicate 22 °C responses and solid symbols 37 °C. The currents were normalized to the largest response of the series. $\alpha_{1A}$ (P/Q-type), $\alpha_{1B}$ (N-type) and $\alpha_{1C}$ (L-type) subunits were expressed in combination with $\beta_{1B}$ and $\alpha_{2\delta}$ subunits. Data shown are the means ± S.E.M. of data obtained from HEK 293 cells expressing L- ($n$ = 8/22, 22/37 °C), P/Q- ($n$ = 8/9) or N-type channels ($n$ = 8/12).

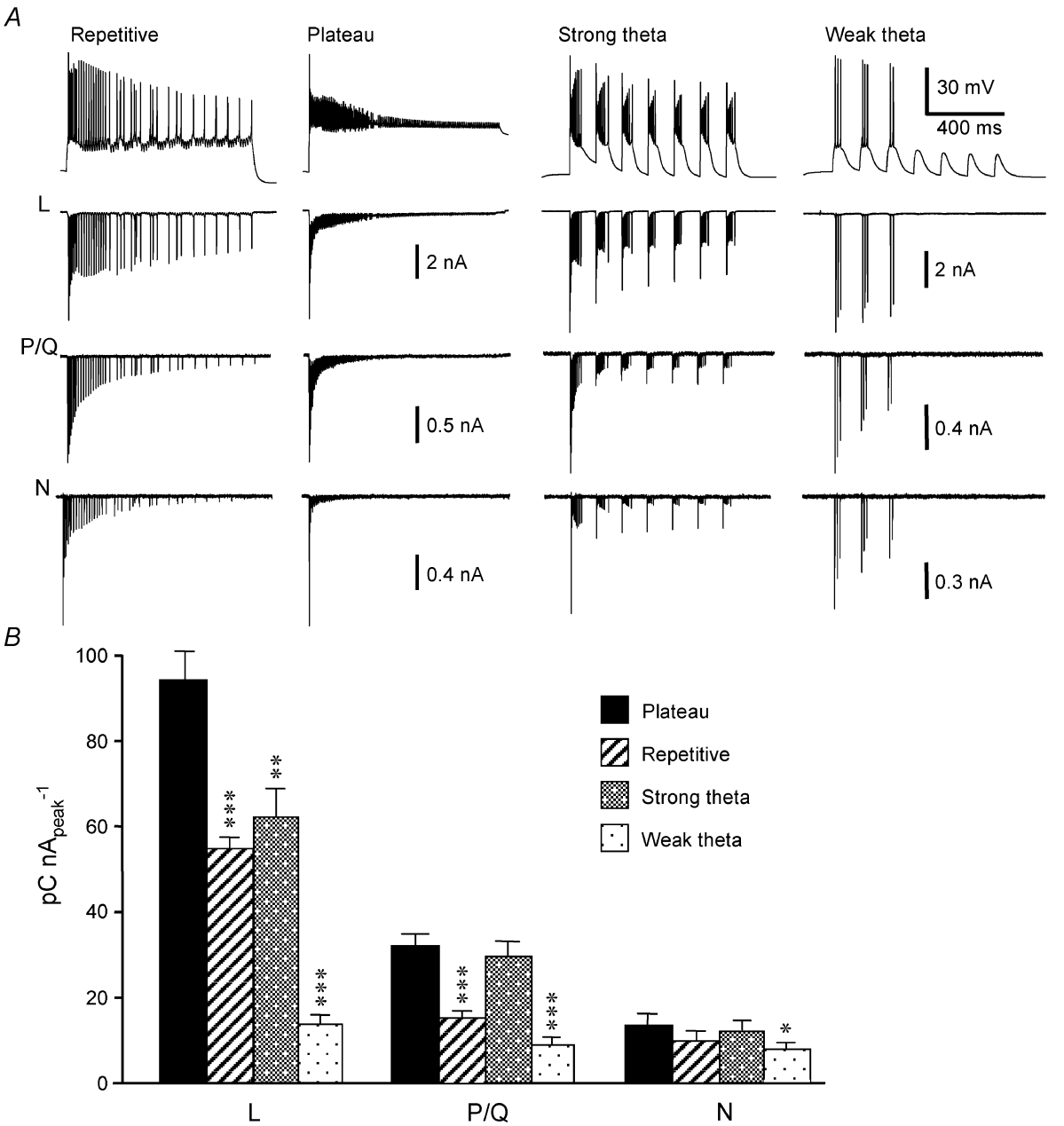


**Figure 2. $Ca^{2+}$ currents in response to simulated waveforms**

*A*, the upper panel shows 1 s duration computer-simulated voltage waveforms used as command potentials to activate the VSCCs (delivered from −70 mV). The lower three panels show the $Ca^{2+}$ current at 37 °C in response to the corresponding voltage waveform above them. *B*, group data for the results shown in *A*. Each column was obtained by integrating the total $Ca^{2+}$ current in response to the corresponding voltage waveform (units pC) and subsequently normalizing this to the peak current response (units nA) of a preceding step depolarization (see Methods; expressed as pC $nA_{peak}^{-1}$). The results indicate a considerably larger integrated $Ca^{2+}$ current mediated by the L-type channel in response to complex voltage waveforms. L-type channel activation in response to the repetitive, plateau, and strong theta waveforms resulted in a significantly larger normalized $Ca^{2+}$ integrated current than that observed from P/Q- or N-type channels ($P < 0.001$; $n > 10$ for all groups). In the case of the weak theta waveform only a modest difference was observed between the L- and P/Q-type channels ($P = 0.037$), while the N-type channel response was significantly smaller ($P < 0.001$). Compared to the other two channel types, L-type VSCCs showed a stronger preference for the plateau waveform than the other 3 waveforms given. We have illustrated this difference (comparison between plateau and other waveforms within a channel type) on the figure using asterisks: * $P < 0.05$; ** $P < 0.01$; *** $P < 0.001$.

small steady drop in baseline, while the P/Q response was associated predominantly with APs at the beginning of the waveform (Figs 2*A* and 3). The N-type channel showed relatively little $Ca^{2+}$ influx in response to the plateau-type waveform with current largely associated with the initial spike. The restriction of the current to the initial spike is probably attributed to channel's closure due to insufficient depolarization (given the channel's more positive activation curve) as well as voltage-dependent inactivation (Fig. 1*C* and *D*). Although the plateau waveform led to a considerably more sustained level of depolarization than the repetitive firing waveform, it produced only a 67 % increase in current for the L-type channel and only 27 % increase for the N-type channel (Fig. 2*B*). This observation suggests that APs and not necessarily large, potentially non-physiological plateau potentials or EPSPs are required to produce effective activation of L-type VSCCs. The ability of the L-type VSCC to become effectively activated by postsynaptic spiking is consistent with a recent report showing that APs alone are sufficient to induce late-phase long-term potentiation (LTP)-related cell signalling (Dudek & Fields, 2002). Interestingly, the difference in integrated current among the L-, P/Q- and N-type VSCCs in response to the complex waveforms (repetitive firing or plateau) was significantly larger than that expected from the response to more simple step depolarization (Figs 1*B,* 2*A* and *B*) indicating that unique channel properties emerge with the more physiological relevant waveforms permitting selective activation. Furthermore, marked temporal differences in the pattern of $Ca^{2+}$ entry was observed between the channels with the complex waveforms. For example, significant $Ca^{2+}$ entry only occurs during the first third of the 1 s stimulus for P/Q- and N-type channels (Fig. 2*A*).

In addition to the 100 Hz tetanic stimulation protocol, we also used a simulated theta rhythm in which the postsynaptic effect of 7.5 Hz presynaptic stimulation was determined. Under conditions with a strong synaptic conductance our model produced a voltage waveform with robust repetitive firing followed by $Na^{+}$ channel inactivation and spike accommodation. With a weaker synaptic conductance only three APs were observed on the first two bursts and two APs on the third (Fig. 2*A* and *B*). Subsequent theta stimuli resulted in EPSPs only. In experiments on HEK 293 cells a significantly larger

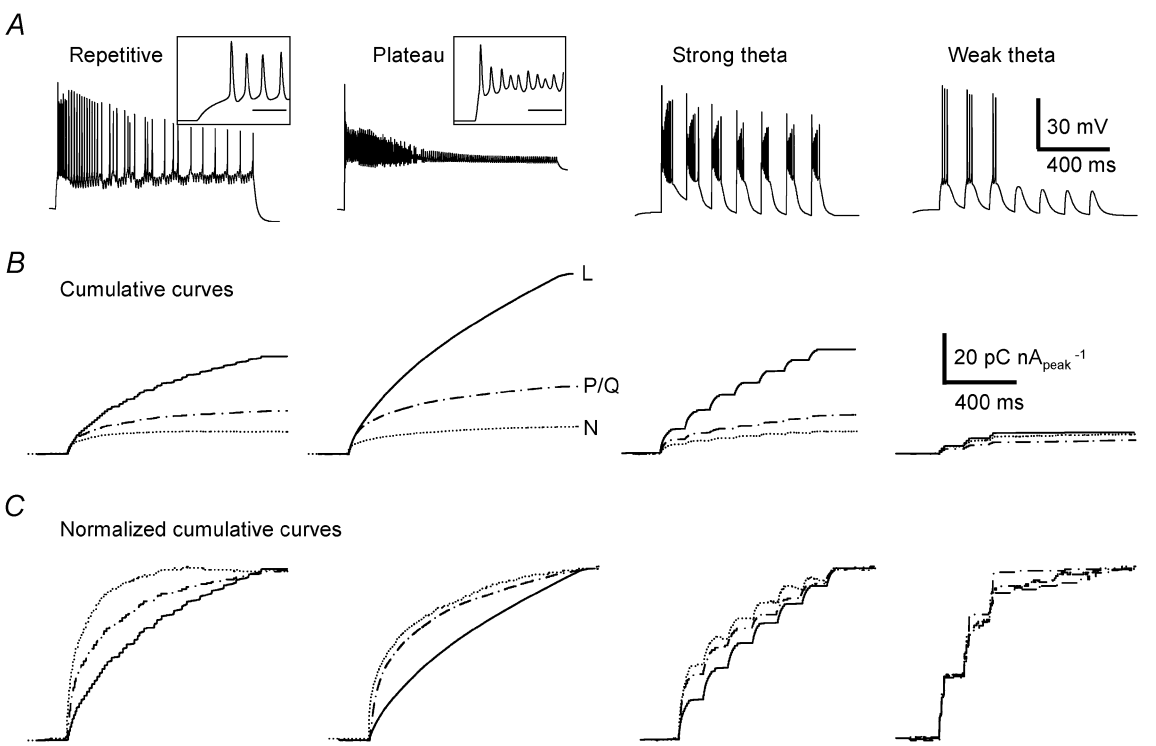


**Figure 3. Cumulative plots of $Ca^{2+}$ currents in response to complex waveforms**

*A*, voltage commands used to evoke the VSCC currents in HEK 293 cells. The inset shows the expanded view of the first firing segment. Calibration bar is 10 ms. *B*, sample cumulative plots of $Ca^{2+}$ currents (total charge) recorded from individual HEK 293 cells expressing L-, P/Q- or N-type VSCCs (using the same current traces as shown in Fig. 2*A*). Responses were normalized to a preceding step pulse as described in the Methods (and employed in Fig. 3*B*) to compare the total charge influx mediated by the different VSCC types. *C*, cumulative current plots normalized to the maximal value permitting a better comparison of response kinetics. Note for N- and P/Q-type channels charge influx was primarily associated with APs. $\alpha_{1A}$ (P/Q-type), $\alpha_{1B}$ (N-type) and $\alpha_{1C}$ (L-type) subunits were expressed in combination with $\beta_{1B}$ and $\alpha_{2\delta}$ subunits.

response of the L-type VSCC (compared to the P/Q- and N-type VSCCs) was observed with the strong theta stimuli but not the weak stimuli (Fig. 2*A* and *B*). Inspection of the individual records revealed that the L-type $Ca^{2+}$ current was largely associated with the APs and was rapidly and reversibly truncated during the $Na^{+}$ channel inactivation (Figs 2*A* and 3*C*). In contrast, examination of the P/Q-type records (strong theta response) revealed an exponential reduction in the AP response (Fig. 2*A*) with each successive AP suggesting that an inactivation process was initiated that proceeded over the course of the additional stimuli. In response to the strong theta waveform the N-type channel current showed an initial rapid decrement in response associated with the first group of high-frequency spikes followed by recovery (within the same burst). A component of the reversible suppression of the N-type response was attributed to this channel's relatively more positive activation voltage ($V_{½}$ = +6 mV at 2 mM $CaCl_2$). Presumably, the truncated action potentials would be of insufficient amplitude to fully activate the N-type channel.

To better evaluate differences in the time course of VSCC activity and to visualize slowly evolving steady inward currents (especially associated with the plateau waveform), we have plotted the cumulative $Ca^{2+}$ current for the three channels examined (Fig. 3*A* and *B*). By normalizing the response of each channel to its total

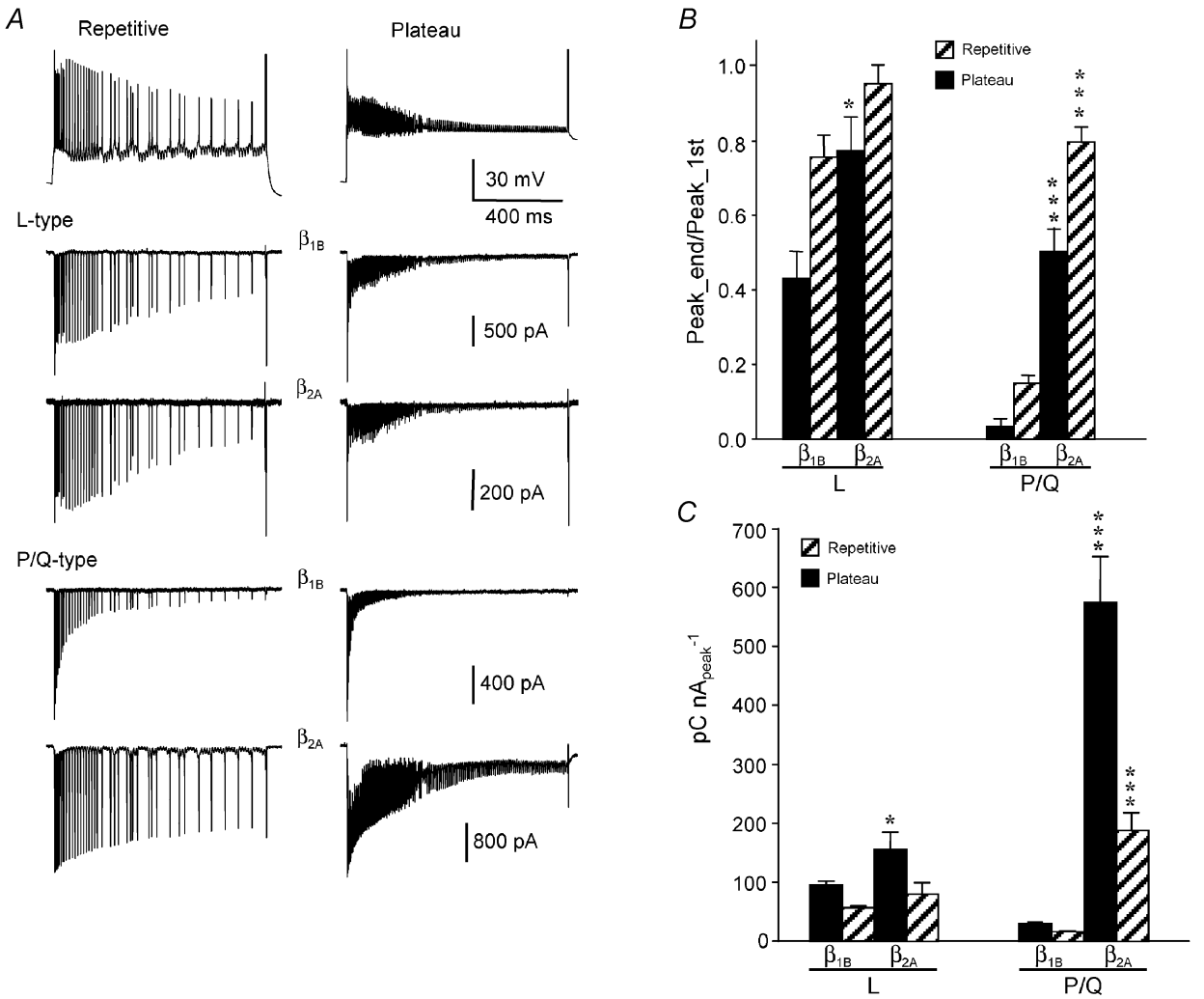


**Figure 4. $\beta$-Subunit expression differentially regulates the response of VSCCs to complex voltage waveforms**

Inactivation was assessed by placing a 5 ms square pulse (to +25 mV) at the end of the train stimulus and comparing its response amplitude (tail $Ca^{2+}$ current ($I_{Ca}$) peak) to the amplitude of the first action potential-induced current at 37 °C in both the repetitive firing and plateau waveforms. *A*, sample traces showing the VSCC current in response to the depolarization waveforms with the 5 ms end-pulses. $\alpha_{1A}$ (P/Q-type) and $\alpha_{1C}$ (L-type) subunits were expressed in combination with $\beta_{1B}$ or $\beta_{2A}$ (as indicated) and $\alpha_{2\delta}$ subunits. *B*, group data showing the ratio of response amplitude (5 ms end-pulse response *versus* that to the first action potential). *C*, group data illustrating the normalized integrated current response for P/Q- and L-type channels expressing either $\beta_{1B}$ or $\beta_{2A}$. * $P < 0.05$; ** $P < 0.01$; *** $P < 0.001$, comparison for a particular channel and waveform with either $\beta_{1B}$ or $\beta_{2A}$: L- ($n$ = 9) and P/Q-type ($n$ = 7).

integrated current (Fig. 3*C*) it was clear that P/Q- and N-type channels contributed the most during the first few 100 ms of the waveforms used. The responses of all three channels to the repetitive firing waveform were largely associated with the AP components and not the steady EPSP component. The use of strong theta burst stimuli indicated a diminishing role of P/Q- and N-type channels with each subsequent burst of a seven-burst train. The use of weak theta train revealed little difference between the three channel types.

### Selective inactivation of P/Q- and N-type voltage sensitive $Ca^{2+}$ channels in response to complex synaptic waveforms

L- and P/Q-type channels are both subject to voltage- and $Ca^{2+}$-dependent inactivation (Yue *et al.* 1990; Lee *et al.* 1999). It is possible that the selective response of the L-type VSCC to the repetitive firing waveforms is a result of P/Q- and N-type channels becoming preferentially inactivated. To test this hypothesis we used a large step depolarization (to 25 mV for 5 ms) at the end of the complex waveform to monitor inactivation (Fig. 4*A*). We observed that a considerably smaller fraction of the P/Q-type VSCCs was available for activation at the end of the waveform compared to the L-type (Fig. 4*A* and *B*). This result was consistent with preferential inactivation of P/Q-type VSCCs contributing to their relatively smaller response to complex voltage waveforms such as the repetitive firing stimulus or the plateau potentials.

To examine the issue of inactivation further, VSCC subunit combinations with reduced voltage-dependent inactivation were expressed (Stotz & Zamponi, 2001). Expression of the $\alpha_{1A}/\beta_{2A}/\alpha_{2\delta}$ subunit combination markedly attenuated the inactivation of P/Q-type channels in response to a 1 s step depolarization to 0 mV at 37 °C (fast decay $\tau$ lengthens from 22.6 ± 1.8 ms, $n = 31$ to 72.8 ± 11.4 ms, $n = 5$, $P < 0.001$; steady-state current level increases from 2.7 ± 0.4 %, $n = 8$ to 32.5 ± 2.6 % of the peak amplitude, $n = 5$, $P < 0.001$; see Table 2). Under these conditions we observed that the P/Q-type VSCC exhibited a very strong response to the complex waveforms (Fig. 4*A*

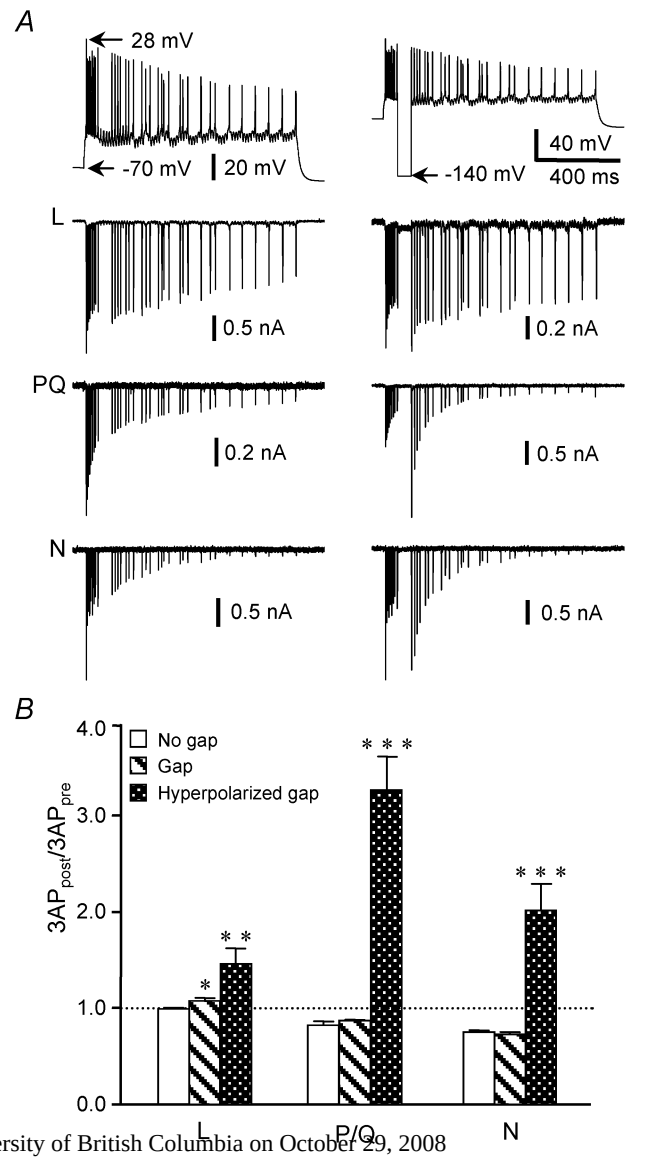


**Figure 5. Differential recovery of VSCCs from inactivation in response to a gap in AP firing**

*A*, the left column shows the $Ca^{2+}$ current in response to the repetitive firing waveform (see Fig. 4*A* for original), with four action potentials removed. During the AP gap (at −45 to −50 mV) the L-type VSCC current recovered while the P/Q- and N-type continued to inactivate. On the right column, the membrane potential during the gap was hyperpolarized to −140 mV leading to marked acceleration of P/Q- and N-type channel recovery from inactivation. *B*, group data illustrating differences in recovery between the channel types in response to the 4-AP gap. Values shown are ratio of the average amplitude of the $Ca^{2+}$ current elicited by three action potentials after the gap *versus* average $Ca^{2+}$ current amplitude for three action potentials before the gap. For L-type VSCCs, both the normal gap waveform (left column) and the −140 mV hyperpolarized gap waveform have significantly increased ratios (1.07 ± 0.03, $n = 9$ and 1.46 ± 0.16, $n = 4$ respectively) compared to normal repetitive firing waveform (0.99 ± 0.01, $n = 9$). For P/Q-type $Ca^{2+}$ channels, removal of 4 APs did not significantly reduce the progressive inactivation (ratios: 0.82 ± 0.04, $n = 5$ and 0.87 ± 0.01, $n = 5$ for the regular repetitive waveform and normal gap waveform respectively). Hyperpolarization to −140 mV greatly accelerated the recovery of the P/Q-type channel from inactivation (3.26 ± 0.35, $n = 8$). This enhanced recovery is significantly more than that observed in the L-type channels ($P = 0.0062$). Similar to the P/Q-type channels, inactivation of the N-type was not attenuated in normal gap waveform (0.73 ± 0.02, $n = 6$) as compared to that in regular repetitive waveforms (0.75 ± 0.02, $n = 8$). The ratio for hyperpolarized gap waveform in N-type channels was also significantly increased (2.01 ± 0.28, $n = 2$). Experiment temperature was 37 °C. Asterisks indicate comparisons to the normal repetitive firing waveform among the same channel type: * $P < 0.05$; ** $P < 0.01$; *** $P < 0.001$. $\alpha_{1A}$ (P/Q-type), $\alpha_{1B}$ (N-type) and $\alpha_{1C}$ (L-type) subunits were expressed in combination with $\beta_{1B}$ and $\alpha_{2\delta}$ subunits.

**Table 2. Decay time course for $Ca^{2+}$ current evoked by 1 s of step depolarization**

| | | $\tau_1$ (ms) | $\tau_1$ (%) | $\tau_2$ (ms) | $\tau_2$ (%) |
|---|---|---|---|---|---|
| 22 °C | | 29.6 ± 1.9 | 45.3 ± 2.3 | 301.5 ± 17.6 | 40.8 ± 2.6 |
| | L | $n = 8$ | $n = 8$ | $n = 8$ | $n = 8$ |
| | | | 295.3 ± 37.6* | | |
| | P/Q | | $n = 11$ | | |
| 37 °C | | 17.8 ± 1.4 | 72.4 ± 2.1 | 207.5 ± 16.2 | 18.5 ± 1.1 |
| | L | $n = 23$ | $n = 23$ | $n = 22$ | $n = 21$ |
| | | 22.6 ± 1.8 | 75.2 ± 2.2 | 172.8 ± 16.0 | 19.0 ± 3.0 |
| | P/Q | $n = 31$ | $n = 26$ | $n = 26$ | $n = 26$ |
| | | 18.1 ± 1.6 | 77.0 ± 3.9 | 270.2 ± 45.7 | 15.1 ± 4.1 |
| | N | $n = 15$ | $n = 14$ | $n = 15$ | $n = 14$ |

All of the decay constants ($\tau$) were significantly reduced by increased temperature ($P < 0.001$). * P/Q-type currents decay with a single exponential component at room temperature. % refers to the percentage of the peak current that was described by each exponential component. $\alpha_{1A}$ (P/Q-type), $\alpha_{1B}$ (N-type) and $\alpha_{1C}$ (L-type) subunits were expressed in HEK 293 cells in combination with $\beta_{1B}$ or $\beta_{2A}$ and $\alpha_{2\delta}$ subunits.

and *C*). In fact the integrated current responses from the P/Q-type ($\alpha_{1A}/\beta_{2A}/\alpha_{2\delta}$) exceeded those of the L-type VSCC indicating that the differential expression of $\beta$ subunits and regulation of $\alpha$ subunits by alternative splicing (Bourinet *et al.* 1999) can have a significant physiological impact on channels expressed. Consistent with the L-type channel having predominantly $Ca^{2+}$-dependent inactivation, expression of L-type channels containing $\beta_{2A}$ did not appreciably alter the integrated currents obtained (as compared to the P/Q-type channel). To examine the role of $Ca^{2+}$-dependent inactivation of L-type channels we substituted $Ba^{2+}$ for $Ca^{2+}$ and found a marked increase in the normalized integrated current when complex waveforms were used (data not shown).

The continuing inactivation observed in P/Q- and N-type channels during the repetitive firing waveform may be partly attributed to the difference in inactivation voltage dependence between L-type and P/Q- or N-type channels, with the L-type channel having a more depolarized inactivation profile. In addition, work by Yue and colleagues suggest (Patil *et al.* 1998) that P/Q- and N-type channels can become inactivated during a relatively hyperpolarized interval between successive depolarizing stimuli. According to this mechanism the channels can enter inactivated states from a closed state thus membrane potentials that lead to inactivation need not necessarily first activate the channel. This form of inactivation is termed intermediate closed-state inactivation and might help explain why P/Q-type channels are selectively inactivated by complex voltage stimuli that contain relatively brief periods of AP depolarization (sufficient to activate the channel) when compared to sustained step depolarization. A similar phenomenon also occurs with $Na^+$ channels and contributes to activity-dependent alterations in dendritic spiking (Colbert *et al.* 1997; Mickus *et al.* 1999). In the case of our VSCC stimuli, the depolarized AP peaks in combination with more moderate EPSPs may be ideal for producing selective inactivation of P/Q- and N-type $Ca^{2+}$ channels. To test this idea we removed four successive APs from the simulated repetitive firing waveform to determine whether inactivation of P/Q-type channels would proceed in the absence of AP stimulation. Our results indicate that the four spikes had little effect on the inactivation of subsequent AP-evoked P/Q-type currents suggesting that the inactivation process once begun could proceed with additional stimulation (Fig. 5*A*). To quantify this effect we measured the average peak current attributed to the three spikes preceding the gap and three after the gap. In the case of the P/Q-type channel a significant reduction in the current amplitude associated with the latter three spikes was observed (−13 ± 1 %, $P < 0.05$ paired $t$ test, $n = 5$) following the four AP gap; while removal of the APs led to an increase in the L-type VSCC response (7 ± 3 %, $P < 0.05$ paired $t$ test, $n = 9$). Similar to the P/Q-type channels, inactivation of the N-type was not attenuated by placing a four AP gap in the waveform as compared to the regular repetitive firing waveforms (−27 ± 2 %, $n = 6$ without and −25 ± 2 %, $n = 8$ with the gap; Fig. 5*B*). Consistent with the idea that voltage-dependent inactivation was important for the apparent difference between the channels, insertion of a hyperpolarized interval (−140 mV) during the AP gap led to a profound facilitation (> 100 % increase) of the AP-evoked $Ca^{2+}$ current mediated by the P/Q- and N-type channels for several 100 ms after the gap (Fig. 5*A* and *B*). Based on previous work the hyperpolarized interval would be expected to speed recovery from inactivation (Patil *et al.* 1998). Although hyperpolarization to −140 mV is not physiological, it nonetheless illustrates the importance of the steady-state membrane potential during the interval between spikes within short trains in determining both the

number of channels available for activation and their recovery from previous inactivation.

The data presented above suggest that the selective response of the different channel types to the repetitive firing waveform could be attributed to the presence of the EPSP component that contributes to preferential voltage-dependent inactivation of P/Q- and N-type channels. To further evaluate this we contrasted the effect of EPSP removal for L-, P/Q- and N-type VSCCs (see example of P/Q data in Fig. 6*A*). Removal of the EPSP component from the stimulus waveform (leaving only APs delivered from −70 mV) resulted in a significant decrease in the integrated $Ca^{2+}$ current via the L-type VSCC and an increase in integrated $Ca^{2+}$ current via the P/Q- and N-type channels (Fig. 6*A* and *B*). Without the EPSP component, the integrated L-type current ($38.5 \pm 2.4$ pC $nA_{peak}^{-1}$, $n = 12$) was still significantly larger than that mediated by P/Q- ($28.5 \pm 3.6$ pC $nA_{peak}^{-1}$, $n = 9$; $P < 0.05$, Fig. 6*B*) or N-type channels ($17 \pm 3$ pC $nA_{peak}^{-1}$, $n = 8$; $P < 0.001$, compare with EPSP-containing value $11 \pm 2$ pC $nA_{peak}^{-1}$, $n = 8$), suggesting that EPSPs in combination with APs produce selective P/Q- and N-type channel inactivation and thus contribute to the privileged response of the L-type VSCC to complex waveforms.

Since the recovery of VSCCs from inactivated states is accelerated by hyperpolarization (Kass & Sanguinetti, 1984; Gutnick *et al.* 1989; Patil *et al.* 1998) (see Fig. 5), we edited our repetitive firing waveform so that the APs would be elicited from an extremely negative potential (−110 mV). APs elicited from this holding potential were associated with significantly larger normalized $Ca^{2+}$ currents for the P/Q- and N-type channels (Fig. 6*B*). For the P/Q-type channel, hyperpolarization to −110 mV largely blocked inactivation as measured by the ratio of the $Ca^{2+}$ current response (last/first AP response; $0.84 \pm 0.05$, $n = 5$). In contrast, the ratio for the normal repetitive firing waveform with approximately a −50 mV interspike potential was significantly lower ($0.11 \pm 0.01$, $n = 9$; $P < 0.001$, see Fig. 2*A* for an example). A repetitive firing waveform lacking EPSPs and with a −70 mV interspike potential had an intermediate ratio when P/Q-type channels were expressed ($0.52 \pm 0.03$, $n = 9$; $P < 0.001$). Hyperpolarization also increased the currents mediated by the N-type channel, although to a lesser extent (ratio of the last AP to first: $0.27 \pm 0.04$, $n = 6$ for −110 mV no EPSP; $0.05 \pm 0.01$, $n = 11$ for the normal repetitive firing waveform; $0.15 \pm 0.02$, $n = 8$ for −70 mV no EPSP). The ability to modulate the degree of VSCC inactivation by the interspike membrane potential provides additional data

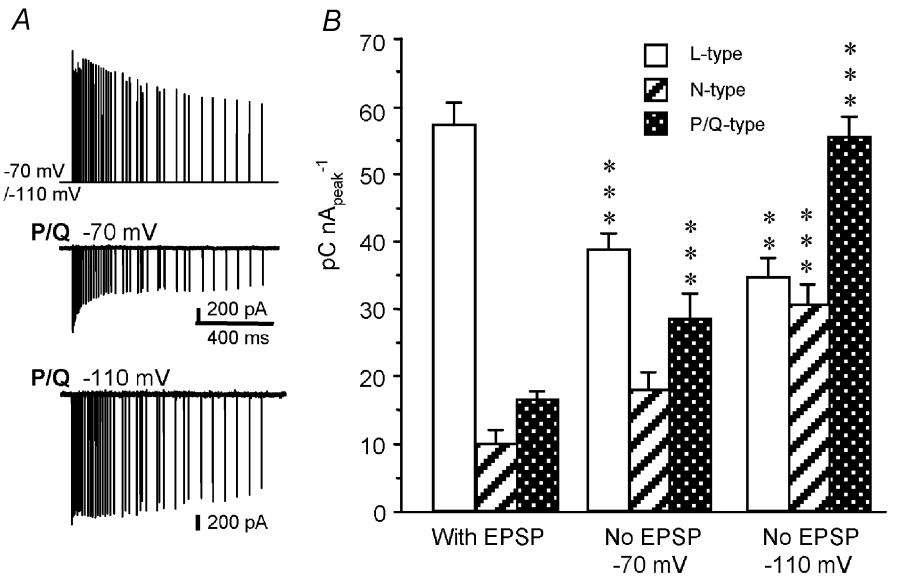


**Figure 6. Differential effect of EPSP removal from complex waveforms on L-type *versus* P/Q- and N-type VSCCs**

*A*, example of $Ca^{2+}$ currents mediated by P/Q-type VSCCs stimulated by the repetitive firing voltage waveform without the EPSP component (centre panel) at 37 °C. Progressive inactivation of the VSCC current in response to AP stimuli was reduced by removal of EPSPs (see Fig. 2*A* for control example with both EPSPs and APs). Hyperpolarization to −110 mV (AP amplitude increased so the peaks are at the same membrane potential) produced a further attenuation of inactivation associated with the AP stimuli. *B*, group data showing the mean normalized integrated VSCC current in response to repetitive firing waveforms with different interspike membrane potentials (−70 or −110 mV for N-, L- and P/Q-type channels). $\alpha_{1A}$ (P/Q-type), $\alpha_{1B}$ (N-type) and $\alpha_{1C}$ (L-type) subunits were expressed in HEK 293 cells in combination with $\beta_{1B}$ and $\alpha_{2\delta}$ subunits. * $P < 0.05$; ** $P < 0.01$; *** $P < 0.001$, comparison by ANOVA between with EPSP (typical repetitive firing waveform) and −70 mV no EPSP or −110 mV no EPSP, the results shown are from $n = 4$–12 cells for each group).

supporting preferential voltage-dependent inactivation as contributing to the waveform preference we observe. In contrast to the P/Q- and N-type channels, the L-type VSCC was relatively unaffected by the interspike membrane potential (ratio of the last AP to first: 0.79 ± 0.09, $n = 4$ for −110 mV; 0.45 ± 0.03, $n = 10$ for normal repetitive; 0.62 ± 0.04, $n = 13$ for −70 mV).

### Recovery from inactivation at physiological temperature

The use of complex waveforms that lack EPSPs indicated that some of the difference in integrated current between L-, P/Q- and N-type channels was due to differences in inactivation triggered by steady depolarization. This is expected since the steady-state inactivation curves were markedly different between the channels (L-type channels are 30 mV more positive; Fig. 1*D*). In addition to reduced inactivation, some of the preferential response of the L-type channel could be attributed to faster recovery from inactivation. To further examine this issue we produced repetitive firing voltage waveforms (containing both EPSPs and APs) with depolarizing test pulses (5 ms step to +25 mV) given at various intervals after the conditioning train (Fig. 7*A* and *B*). The amplitude of the test pulses was compared to that of a pulse given before the repetitive firing waveform. Comparison of the three channel types indicated that the P/Q-type channel showed markedly slower recovery from inactivation than the L- or N-type channels (Fig. 7*B*). Using a different inactivation protocol with 1 s of sustained depolarization to 0 mV we found that a slow component of recovery (> 1 s, ~25 %) was also observed for all three channel types.

## DISCUSSION

In this study we have focused on the activation of high threshold $Ca^{2+}$ channels by physiologically relevant voltage waveforms. Our emphasis has been on contrasting the response of L-, P/Q- and N-type channels. We have expressed L-type channels composed of $\alpha_{1C}$ subunits that recent data from hippocampal neurons suggest are predominantly involved in coupling depolarization to activation of gene transcription factor cAMP-response element binding protein (CREB)-dependent gene expression (Weick *et al.* 2003). It should be stressed that L-type channels can also be composed of $\alpha_{1D}$ subunits that have been shown to constitute a component of the L-type current in neurons (Hell *et al.* 1993). However, $\alpha_{1D}$ (in contrast to $\alpha_{1C}$) does not appear to couple to intracellular effectors such as PDZ-domain-containing proteins (Weick *et al.* 2003) that are required for efficient L-type channel-dependent stimulus–transcription coupling and therefore we have focused our study on $\alpha_{1C}$ containing channels.

Our data show that at physiological temperature, L-, P/Q- and N-type VSCCs all exhibit markedly enhanced activation, inactivation and peak current amplitude compared to room temperature. At room temperature all three channels require a significantly longer duration of

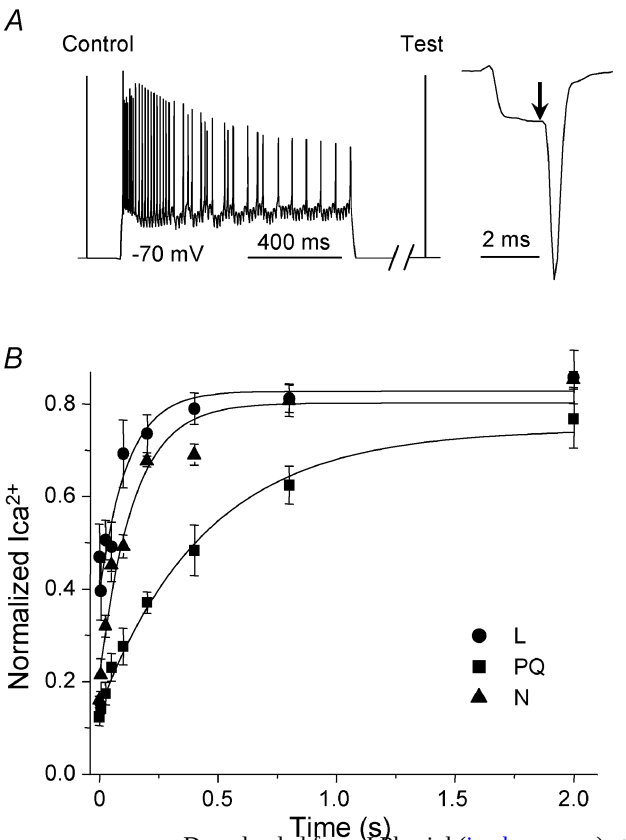


**Figure 7. Recovery from inactivation induced by complex voltage waveforms**

*A*, the repetitive firing voltage waveform as described in the previous figures, was preceded by a +25 mV control pulse and followed at varied intervals by a +25 mV test pulse. The current record on the right indicates how the control or test pulse evoked $Ca^{2+}$ current was monitored at 37 °C. The point at which the current amplitude was measured (steady-state component, not tail current) is indicated by the arrow. *B*, plots of the normalized (to control pulse) recovery of test pulse amplitude (means ± S.E.M.) at varying intervals after the repetitive firing voltage waveform. The data was fitted to a single exponential function with an offset reflecting the degree of starting inactivation. The P/Q time constant ($\tau = 450 \pm 77$ ms, $n = 6$) was considerably longer than that derived for the L- (117 ± 24 ms, $n = 5$) or N-type (141 ± 21 ms, $n = 5$) VSCC. A minor slower component of recovery from inactivation with a $\tau > 2000$ ms was also observed (~20 %). $\alpha_{1A}$ (P/Q-type), $\alpha_{1B}$ (N-type) and $\alpha_{1C}$ (L-type) subunits were expressed in HEK 293 cells in combination with $\beta_{1B}$ and $\alpha_{2\delta}$ subunits.

depolarization to become activated than that required at 37 °C. Thus, at reduced temperature (22 °C) it is possible that conditions that alter AP duration such as the modulation of $K^+$ channels would change both the degree and duration of channel activation (Sabatini & Regehr, 1997). The rapid activation of L-type VSCCs with stimuli resembling single APs we observed is consistent with previous pharmacological data showing a role for the L-type channel in AP-mediated $Ca^{2+}$ transients (Christie *et al.* 1995*a*). The effective activation of L-type VSCCs by APs alone (without a requirement for EPSPs) indicates that specific frequencies of postsynaptic spiking may be an effective means of activating events associated with late phase long-term potentiation, consistent with recent findings (Dudek & Fields, 2002). However, it is likely that EPSPs in combination with APs are required to tag and strengthen specific synapses (Deisseroth *et al.* 1996; Frey & Morris, 1997). Although EPSPs may be required for triggering local chemical events (perhaps through NMDA-receptor-mediated $Ca^{2+}$ influx) they are actually relatively inefficient at activating VSCCs even when of large amplitude. To address this more quantitatively we asked what was the best way to activate VSCCs (measured by integrated current over 1 s if given the ability to deliver 100 ms of depolarization from a −70 mV holding potential in different ways over a period of up to 1 s (data not shown)). For example, what provides more integrated VSCC current, 100 1 ms steps to 0 mV (given over 1 s) or 100 ms of continuous depolarization? Other combinations are also possible 10 10 ms steps or 333 0.3 ms steps. Surprisingly steps resembling actual action potentials (half-widths of ~1 ms) were more effective at activating L- and P/Q-type channels. The reasons for this are easy to understand and include: little inactivation associated with 1 ms pulses and a high proportion of the current appearing as a tail current (having a larger driving force). Pulses of shorter duration (0.3 ms) are expected to be less effective since they would fail to fully activate the channels (Fig. 1*F*). Thus the activation and inactivation rates for high threshold VSCCs are tuned to the properties (amplitude and shape) of the AP and not necessarily long lasting EPSPs.

Our data indicating that APs are the most effective means of activating recombinant L-type VSCCs would seem to be in contradiction to recent data from us and others showing that L-type channels have a preference for large EPSPs over APs (Nakazawa & Murphy, 1999; Mermelstein *et al.* 2000). There are several potential explanations for this including the fact that the EPSPs used in these studies were prolonged step depolarizations to −30 to −15 mV and were not necessarily physiologically relevant waveforms. Given the steady-state inactivation curves of the L-, P/Q- and N-type channels (Fig. 1), it is possible that the waveforms selectively inactivated P/Q- and N-type channels. Furthermore, these waveforms only contained a single AP as opposed to 40–50 spikes contained in some of the waveforms used in this study. Previous observations that are more difficult to reconcile with the current data are why L-type VSCCs mediate only a relatively small fraction of the $Ca^{2+}$ response to single APs (Nakazawa & Murphy, 1999; Mermelstein *et al.* 2000). Potentially this finding can be explained if the relative abundance as well as the waveform preference of L-type *versus* other VSCCs is considered. For example, if only 20 % of the VSCCs are L-type (defined by peak current amplitude in response to a step, as in Fig. 1), then assuming equal activation of all VSCC types we would expect 20 % of the AP-evoked $Ca^{2+}$ transient to be blocked by a (L-type) dihydropyridine antagonist. In the case of the complex waveforms (such as the repetitive firing one we used) a factor related to waveform preference needs to be considered when evaluating the responses between channel types to different waveforms. Assuming the L-type has an abundance of only 20 %, but results in an integrated current that is three times larger (waveform preference factor) with the repetitive firing waveform relative to the P/Q- and N-type, the responses to complex waveforms can be estimated as follows: 0.20 L-abundance × 3.0 L-preference = 0.6 L-response; *versus* 0.8 non-L-abundance × 1.0 non-L-preference = 0.8 non-L-response. Therefore addition of an L-type VSCC specific dihydropyridine antagonist could block 43 % of the repetitive firing induced $Ca^{2+}$ transient (fraction L = 0.6 L/(1.4 total L + non-L)), but only 20 % of the single AP response similar to previous reports using mixed populations of channels (Nakazawa & Murphy, 1999; Mermelstein *et al.* 2000).

Although closely functionally related channels such as the P/Q-type (with the inactivating $\beta_{1B}$ subunit expressed) respond similarly to the L-type VSCC when given 1 s step depolarization, they are selectively inactivated in response to more physiological waveforms, providing a mechanism to discriminate different voltage waveforms created by unique synaptic stimuli. The preferential response of the L-type channel to complex synaptic bursting was attributed to the P/Q- and N-type channels containing $Ca^{2+}$ channel $\beta$ subunits that support voltage-dependent inactivation. Forebrain neurons have been reported to predominantly express the $\beta_{1B}$ isoform suggesting that P/Q-, N-type and other high threshold VSCCs that are subject to voltage-dependent inactivation would be selectively inactivated by the complex waveforms we have used (Ludwig *et al.* 1997). The voltage-dependent inactivation of the P/Q- and N-type channels were facilitated by steady depolarization in the form of EPSPs. In contrast, removal of EPSPs and holding the cell at very negative potentials (−110 mV) completely blocked the inactivation process. These findings highlight important differences for regulation of these channels in dendritic and axonal compartments

where large differences in interspike membrane potential may be present. In the axon the P/Q- and N-type channels would not experience EPSPs and would have a more negative interspike membrane potential greatly reducing inactivation with trains of stimuli and thus increasing the reliability of transmission. In contrast, in the soma and dendrites EPSPs would help to inactivate non-L-type VSCCs (P/Q and N) and leave a response mediated predominantly by L-type channels. For L-type VSCCs that are subject to primarily $Ca^{2+}$-dependent inactivation, the local intracellular $Ca^{2+}$-handling environment is likely to influence waveform preference and could account for why sustained depolarization (1 s step to 0 mV) leads to relatively more L-type VSCC inactivation than the repetitive AP/EPSP waveform. Given that the various classes of VSCCs have different kinetics and mechanisms of inactivation it is tempting to imagine scenarios in which particular VSCCs are tuned to specific stimuli based on their inactivation and recovery kinetics. The ability of relatively low amplitude steady depolarization (i.e. to −55 mV) to influence the number of P/Q- and N-type channels available for activation without actually activating them provides a powerful mechanism for previous experience to modulate channel function. In contrast, L-type channels would be relatively insensitive to small voltage changes. Since P/Q- and N-type channels exhibit greatly accelerated recovery from inactivation in response to hyperpolarization, it is possible that if the hyperpolarized interval between bursts were longer than the recovery time these channels could be tuned to a particular frequency if given hyperpolarized intervals that are longer than recovery time. The presence of slow $Ca^{2+}$-activated $K^+$ channels might provide hyperpolarization of sufficient duration and magnitude (to −80 mV) to relieve a significant amount of P/Q- and N-type inactivation. Alternatively, other factors within bursting voltage waveforms such as the presence of slow $Na^+$ channel inactivation that lead to spikes of diminishing amplitude would favour the activation of L- and P/Q-type channels which are activated at more negative potentials than N-type channels. This phenomenon would be particularly apparent in dendrites where slow $Na^+$ channel inactivation is most apparent (Colbert *et al.* 1997; Mickus *et al.* 1999). In addition to AP amplitude, other mechanisms may be at work in dendrites to result in more selective VSCC activation with trains of stimuli. For example, although high-voltage activated $Ca^{2+}$ channels are similarly activated with APs of brief duration (< 1 ms), the longer AP duration and greater EPSP amplitude found in distal dendrites (Stuart *et al.* 1997*a*; Magee & Cook, 2000) may promote the selective inactivation of P/Q- and N-type channels. Although we have stressed that L-type VSCCs can be differentially tuned to voltage waveforms we should point out that not all neurons or their associated subcellular components have a large fraction of L-type current (El Manira & Bussieres, 1997; Barnes-Davies *et al.* 2001). In these neurons different $\beta$ subunit expression may determine whether P/Q- and N-type channels can respond to complex waveforms similar to the ones we have used.

In conclusion, we propose that in response to complex synaptic bursting waveforms of long duration P/Q- and N-type channels undergo selective inactivation leading to a $Ca^{2+}$ current mediated predominantly by L-type channels providing a mechanism that works in combination with local chemical events (Deisseroth *et al.* 1996; Dolmetsch *et al.* 2001; Weick *et al.* 2003) to couple these channels to specific tasks such as activity-dependent gene expression (Nguyen *et al.* 1994). However we emphasize that these results from heterologously expressed $Ca^{2+}$ channels need to be repeated in actual hippocampus neurons since a variety of factors including $\alpha_1$ splice variants, $\beta$ subunit expression, and interacting proteins can potentially influence channel kinetics. In addition, VSCC behaviour can even vary within a neuron as channels on neuritic branches can have different properties from those expressed at the soma (Egorov *et al.* 1999; Li *et al.* 2001). Thus it is thus possible that subcellular differences in VSCC structure combined with compartment specific changes in voltage also contribute to selective coupling between synaptic stimuli and VSCC activity.

## REFERENCES

Bading H, Ginty DD & Greenberg ME (1993). Regulation of gene expression in hippocampal neurons by distinct calcium signaling pathways. *Science* **260**, 181–186.

Barnes-Davies M, Owens S & Forsythe ID (2001). Calcium channels triggering transmitter release in the rat medial superior olive. *Hear Res* **162**, 134–145.

Bourinet E, Soong TW, Sutton K, Slaymaker S, Mathews E, Monteil A, Zamponi GW, Nargeot J & Snutch TP (1999). Splicing of alpha 1A subunit gene generates phenotypic variants of P- and Q-type calcium channels. *Nat Neurosci* **2**, 407–415.

Christie BR, Eliot LS, Ito K, Miyakawa H & Johnston D (1995*a*). Different $Ca^{2+}$ channels in soma and dendrites of hippocampal pyramidal neurons mediate spike-induced $Ca^{2+}$ influx. *J Neurophysiol* **73**, 2553–2557.

Christie BR, Stellwagen D & Abraham WC (1995*b*). Reduction of the threshold for long-term potentiation by prior theta- frequency synaptic activity. *Hippocampus* **5**, 52–59.

Colbert CM, Magee JC, Hoffman DA & Johnston D (1997). Slow recovery from inactivation of $Na^+$ channels underlies the activity-dependent attenuation of dendritic action potentials in hippocampal CA1 pyramidal neurons. *J Neurosci* **17**, 6512–6521.

Colbert CM & Pan E (2002). Ion channel properties underlying axonal action potential initiation in pyramidal neurons. *Nat Neurosci* **5**, 533–538.

Deisseroth K, Bito H & Tsien RW (1996). Signaling from synapse to nucleus: postsynaptic CREB phosphorylation during multiple forms of hippocampal synaptic plasticity. *Neuron* **16**, 89–101.

## APPENDIX

**Table 3. Distribution of ionic channels in the NEURON model**

| Channel | Dendrite (distal) | Dendrite (proximal) mS $cm^{-2}$ | Soma mS $cm^{-2}$ | Hillock mS $cm^{-2}$ | Axon mS $cm^{-2}$ | Source of model and conductance level |
|---|---|---|---|---|---|---|
| Na | 15 mS $cm^{-2}$ | 15 | 15 | 300 | 15 | (Destexhe *et al.* 1994; Mainen & Sejnowski, 1998) |
| NaP | 0.02 mS $cm^{-2}$ | 0.05 | 0.1 | 0.1 | — | Maximum conductance on the dendrites was adjusted to obtain proper excitability of the model cell (Lipowsky *et al.* 1996) |
| $K_{dr}$ | 3 mS $cm^{-2}$ | 3 | 3 | 60 | 3 | (Mainen & Sejnowski, 1998) |
| $K_A$ | 7 + 11*(distance from soma in $\mu$m/100) (mS $cm^{-2}$) | 7 | 7 | — | — | (Hoffman *et al.* 1997) |
| $K_M$ | 0.2 mS $cm^{-2}$ | 0.2 | 0.2 | 0.4 | — | Adjusted to balance NaP at resting membrane potential (Mainen & Sejnowski, 1998) |
| $K_{BK}$ | — | 0.2 | 0.2 | 0.1 | 0.8 | (Lipowsky *et al.* 1996) |
| $sI_{AHP}$ | — | 0.2 | 0.2 | 0.2 | | (Sah & Bekkers, 1996) |
| $K_{SK}$ | — | 0.1 | 0.1 | 0.1 | 0.3 | (Lipowsky *et al.* 1996) |
| $Ca_L$ | — | — | 2.5 | 2.5 | — | (Mermelstein *et al.* 2000) |
| NMDA | 0.0075–0.3 $\mu$S | — | — | — | — | Adjusted to represent different levels of synaptic stimulation (Destexhe *et al.* 1994) |
| AMPA | 0.0075–0.3 $\mu$S | — | — | — | — | — |

For simplicity there are three synapses, two on the distal dendrites and one on proximal dendrite. The synaptic conductances (NMDA and AMPA) were adjusted in simulations as needed. The above distribution of ionic channels is for nonbursting cells. For bursting cells, there is more NaP (persistent $Na^+$ channels) (0.1 mS $cm^{-2}$ on proximal dendrites, 0.05 mS $cm^{-2}$ on distal dendrites).


Destexhe A, Mainen ZF & Sejnowski TJ (1994). Synthesis of models for excitable membranes, synaptic transmission and neuromodulation using a common kinetic formalism. *J Comput Neurosci* **1**, 195–230.

Dolmetsch RE, Pajvani U, Fife K, Spotts JM & Greenberg ME (2001). Signaling to the nucleus by an L-type calcium channel–calmodulin complex through the MAP kinase pathway. *Science* **294**, 333–339.

Dudek SM & Fields RD (2002). Somatic action potentials are sufficient for late-phase LTP-related cell signaling. *Proc Natl Acad Sci U S A* **99**, 3962–3967.

Egorov AV, Gloveli T & Muller W (1999). Muscarinic control of dendritic excitability and Ca(2+) signaling in CA1 pyramidal neurons in rat hippocampal slice. *J Neurophysiol* **82**, 1909–1915.

El Manira A & Bussieres N (1997). Calcium channel subtypes in lamprey sensory and motor neurons. *J Neurophysiol* **78**, 1334–1340.

Ertel EA, Campbell KP, Harpold MM, Hofmann F, Mori Y, Perez-Reyes E, Schwartz A, Snutch TP, Tanabe T, Birnbaumer L, Tsien RW & Catterall WA (2000). Nomenclature of voltage-gated calcium channels [letter]. *Neuron* **25**, 533–535.

Fleidervish IA, Friedman A & Gutnick MJ (1996). Slow inactivation of $Na^+$ current and slow cumulative spike adaptation in mouse and guinea-pig neocortical neurones in slices (published erratum appears in *J Physiol* (1996) **494**, 907). *J Physiol* **493**, 83–97.

Frey U & Morris RG (1997). Synaptic tagging and long-term potentiation. *Nature* **385**, 533–536.

Gutnick MJ, Lux HD, Swandulla D & Zucker H (1989). Voltage-dependent and calcium-dependent inactivation of calcium channel current in identified snail neurones. *J Physiol* **412**, 197–220.

Halliwell JV & Adams PR (1982). Voltage-clamp analysis of muscarinic excitation in hippocampal neurons. *Brain Res* **250**, 71–92.

Hell JW, Westenbroek RE, Warner C, Ahlijanian MK, Prystay W, Gilbert MM, Snutch TP & Catterall WA (1993). Identification and differential subcellular localization of the neuronal class C and class D L-type calcium channel alpha 1 subunits. *J Cell Biol* **123**, 949–962.

Hines ML & Carnevale NT (1997). The NEURON simulation environment. *Neural Comput* **9**, 1179–1209.

Hoffman DA, Magee JC, Colbert CM & Johnston D (1997). $K^+$ channel regulation of signal propagation in dendrites of hippocampal pyramidal neurons. *Nature* **387**, 869–875.

Kass RS & Sanguinetti MC (1984). Inactivation of calcium channel current in the calf cardiac Purkinje fiber. Evidence for voltage- and calcium-mediated mechanisms. *J Gen Physiol* **84**, 705–726.

Lee A, Wong ST, Gallagher D, Li B, Storm DR, Scheuer T & Catterall WA (1999). $Ca^{2+}$/calmodulin binds to and modulates P/Q-type calcium channels. *Nature* **399**, 155–159.

Li W, Thaler C & Brehm P (2001). Calcium channels in *Xenopus* spinal neurons differ in somas and presynaptic terminals. *J Neurophysiol* **86**, 269–279.

Lipowsky R, Gillessen T & Alzheimer C (1996). Dendritic $Na^+$ channels amplify EPSPs in hippocampal CA1 pyramidal cells. *J Neurophysiol* **76**, 2181–2191.

Ludwig A, Flockerzi V & Hofmann F (1997). Regional expression and cellular localization of the alpha1 and beta subunit of high voltage-activated calcium channels in rat brain. *J Neurosci* **17**, 1339–1349.

McCobb DP & Beam KG (1991). Action potential waveform voltage-clamp commands reveal striking differences in calcium entry via low and high voltage-activated calcium channels. *Neuron* **7**, 119–127.

Magee JC & Cook EP (2000). Somatic EPSP amplitude is independent of synapse location in hippocampal pyramidal neurons. *Nat Neurosci* **3**, 895–903.

Mainen ZF & Sejnowski TJ. (1998). Modeling active dendritic processes in pyramidal neurons. In *Methods in Neural Modeling,* ed. Koch C & Segev I. MIT Press, Cambridge, MA, USA.

Mermelstein PG, Bito H, Deisseroth K & Tsien RW (2000). Critical dependence of cAMP response element-binding protein phosphorylation on L-type calcium channels supports a selective response to EPSPs in preference to action potentials. *J Neurosci* **20**, 266–273.

Mickus T, Jung H & Spruston N (1999). Properties of slow, cumulative sodium channel inactivation in rat hippocampal CA1 pyramidal neurons. *Biophys J* **76**, 846–860.

Murphy TH, Worley PF & Baraban JM (1991). L-type voltage-sensitive calcium channels mediate synaptic activation of immediate early genes. *Neuron* **7**, 625–635.

Nakazawa H & Murphy TH (1999). Activation of nuclear calcium dynamics by synaptic stimulation in cultured cortical neurons. *J Neurochem* **73**, 1075–1083.

Nguyen PV, Abel T & Kandel ER (1994). Requirement of a critical period of transcription for induction of a late phase of LTP. *Science* **265**, 1104–1107.

Patil PG, Brody DL & Yue DT (1998). Preferential closed-state inactivation of neuronal calcium channels. *Neuron* **20**, 1027–1038.

Pragnell M, Sakamoto J, Jay SD & Campbell KP (1991). Cloning and tissue-specific expression of the brain calcium channel beta-subunit. *FEBS Lett* **291**, 253–258.

Randall A & Tsien RW (1995). Pharmacological dissection of multiple types of $Ca^{2+}$ channel currents in rat cerebellar granule neurons. *J Neurosci* **15**, 2995–3012.

Sabatini BL & Regehr WG (1997). Control of neurotransmitter release by presynaptic waveform at the granule cell to Purkinje cell synapse. *J Neurosci* **17**, 3425–3435.

Sah P & Bekkers JM (1996). Apical dendritic location of slow afterhyperpolarization current in hippocampal pyramidal neurons: implications for the integration of long-term potentiation. *J Neurosci* **16**, 4537–4542.

Shao LR, Halvorsrud R, Borg-Graham L & Storm JF (1999). The role of BK-type $Ca^{2+}$-dependent $K^+$ channels in spike broadening during repetitive firing in rat hippocampal pyramidal cells. *J Physiol* **521**, 135–146.

Spruston N, Schiller Y, Stuart G & Sakmann B (1995). Activity-dependent action potential invasion and calcium influx into hippocampal CA1 dendrites. *Science* **268**, 297–300.

Stocker M, Krause M & Pedarzani P (1999). An apamin-sensitive $Ca^{2+}$-activated $K^+$ current in hippocampal pyramidal neurons. *Proc Natl Acad Sci U S A* **96**, 4662–4667.

Storm J & Hvalby O (1985). Repetitive firing of CA1 hippocampal pyramidal cells elicited by dendritic glutamate: slow prepotentials and burst-pause pattern. *Exp Brain Res* **60**, 10–18.

Stotz SC & Zamponi GW (2001). Structural determinants of fast inactivation of high voltage-activated Ca(2+) channels. *Trends Neurosci* **24**, 176–181.

Stuart G, Schiller J & Sakmann B (1997*a*). Action potential initiation and propagation in rat neocortical pyramidal neurons. *J Physiol* **505**, 617–632.

Stuart G, Spruston N, Sakmann B & Hausser M (1997*b*). Action potential initiation and backpropagation in neurons of the mammalian CNS. *Trends Neurosci* **20**, 125–131.

Sutton KG, McRory JE, Guthrie H, Murphy TH & Snutch TP (1999). P/Q-type calcium channels mediate the activity-dependent feedback of syntaxin-1A. *Nature* **401**, 800–804.

Tateyama M, Zong S, Tanabe T & Ochi R (2001). Properties of voltage-gated Ca(2+) channels in rabbit ventricular myocytes expressing Ca(2+) channel alpha(1E) cDNA. *Am J Physiol Cell Physiol* **280**, C175–182.

Thomas MJ, Watabe AM, Moody TD, Makhinson M & O'Dell TJ (1998). Postsynaptic complex spike bursting enables the induction of LTP by theta frequency synaptic stimulation. *J Neurosci* **18**, 7118–7126.

Tottene A, Moretti A & Pietrobon D (1996). Functional diversity of P-type and R-type calcium channels in rat cerebellar neurons. *J Neurosci* **16**, 6353–6363.

Weick JP, Groth RD, Isaksen AL & Mermelstein PG (2003). Interactions with PDZ proteins are required for L-type calcium channels to activate cAMP response element-binding protein-dependent gene expression. *J Neurosci* **23**, 3446–3456.

Yeckel MF, Kapur A & Johnston D (1999). Multiple forms of LTP in hippocampal CA3 neurons use a common postsynaptic mechanism. *Nat Neurosci* **2**, 625–633.

Yue DT, Backx PH & Imredy JP (1990). Calcium-sensitive inactivation in the gating of single calcium channels. *Science* **250**, 1735–1738.

Zhang JF, Randall AD, Ellinor PT, Horne WA, Sather WA, Tanabe T, Schwarz TL & Tsien RW (1993). Distinctive pharmacology and kinetics of cloned neuronal $Ca^{2+}$ channels and their possible counterparts in mammalian CNS neurons. *Neuropharmacology* **32**, 1075–1088.

Zhong H, Li B, Scheuer T & Catterall WA (2001). Control of gating mode by a single amino acid residue in transmembrane segment IS3 of the N-type $Ca^{2+}$ channel. *Proc Natl Acad Sci U S A* **98**, 4705–4709.

**Acknowledgements**

We thank Dr Terry Snutch for the gift of VSCC clones, the N-type VSCC stable cell line and for technical advice. We thank Brian Christie, Yo Otsu and Lynn Raymond for comments on the manuscript. This work was supported by an operating grant from the CIHR of Canada (MOP-12675). T.H.M. is a CIHR investigator and a MSFHR Senior Scholar.

**Supplementary material**

The online version of this paper can be found at:

DOI: 10.1113/jphysiol.2003.051110

and contains material entitled:

Digital versions of the voltage clamp stimulus waveforms used in the paper (repetitive, plateau, strong theta and weak theta; see Fig. 2).